

Direct Laser Writing of Superhydrophobic PDMS Elastomers for Controllable Manipulation via Marangoni Effect

Wei Wang, Yu-Qing Liu, Yan Liu, Bing Han, Huan Wang, Dong-Dong Han, Jian-Nan Wang, Yong-Lai Zhang,* and Hong-Bo Sun*

Direct light-to-work conversion enables manipulating remote devices in a contactless, controllable, and continuous manner. Although some pioneering works have already proven the feasibility of controlling devices through light-irradiation-induced surface tension gradients, challenges remain, including the flexible integration of efficient photothermal materials, multifunctional structure design, and fluidic drag reduction. This paper reports a facile one-step method for preparing light-driven floating devices with functional surfaces for both light absorption and drag reduction. The direct laser writing technique is employed for both arbitrary patterning and surface modification. By integrating the functional layer at the desired position or by designing asymmetric structures, three typical light-driven floating devices with fast linear or rotational motions are demonstrated. Furthermore, these devices can be driven by a variety of light sources including sunlight, a filament lamp, or laser beams. The approach provides a simple, green, and cost-effective strategy for building functional floating devices and smart light-driven actuators.

1. Introduction

Recently, considerable research effort has been devoted to self-propelled machines due to their broad potential applications such as mechanical devices,^[1,2] automated systems,^[3] sensors,^[4,5] lab-on-a-chip systems, and robotics.^[6–14] To activate such

smart devices, a variety of energy sources such as magnetic fields,^[15–17] light,^[18–20] heat, and humidity has been employed to induce controllable movement.^[21–23] Among these driving strategies, direct light-to-work conversion is a highly attractive option because light is a clean, safe energy source; in addition, light can be transmitted to target objects without physical contact, thus enabling remote control.^[8,24,25] Light-mediated manipulation can be realized based on different driving mechanisms. Typical strategies include optical trapping,^[26] photochemical effects (e.g., photoisomerization, photodimerization),^[27,28] photothermal effects (e.g., photothermal expansion, surface tension, and phase transition), and photoelectric conversion.^[8,19,29–31]

The photothermal surface tension effect is considered an effective driving strategy,^[32] since it enables direct light-to-work conversion independent of environment stimuli and special materials. According to the Marangoni effect,^[33–35] a liquid with a high surface tension pulls more strongly on the surrounding liquid than that with a low surface tension. Based on this basic principle, light has been employed to generate thermal surface tension gradients at a desired position, thus causing a floating object to migrate away from low surface tension regions. For example, Okawa et al. reported surface-tension-mediated photothermal manipulation in 2009.^[19] In their work, a macroscopic vertically aligned carbon nanotube forests (VANTs)-modified polydimethylsiloxane (PDMS) block floating on water was prepared. When a focused pointing light irradiated a part of VANTs, the object was pulled away since the surface tension of water at the irradiated position was greatly reduced. Linear and rotational motions have been demonstrated by selectively focusing light on different regions of the VANTs. Furthermore, the photothermal surface tension effect is also operational at the micro-nanoscale. Maggi et al. developed asymmetric microgears with a uniform layer of amorphous carbon on one side for increased light absorption.^[1] The microgears sit on the liquid–air interface and can efficiently convert absorbed light into rotational motion since the surface tension gradients along the gear's contour would result in a nonzero total torque. The photothermal surface tension effect opens up

W. Wang, Y.-Q. Liu, B. Han, Dr. H. Wang, D.-D. Han, J.-N. Wang, Prof. Y.-L. Zhang, Prof. H.-B. Sun
State Key Laboratory on Integrated Optoelectronics
College of Electronic Science and Engineering
Jilin University
2699 Qianjin Street, Changchun 130012, China
E-mail: yonglaizhang@jlu.edu.cn; hbsun@jlu.edu.cn

Prof. Y. Liu
Key Laboratory of Bionic Engineering (Ministry of Education)
Jilin University
Changchun 130022, China
Prof. H.-B. Sun
College of Physics
Jilin University
Changchun 130012, China

 The ORCID identification number(s) for the author(s) of this article can be found under <https://doi.org/10.1002/adfm.201702946>.

DOI: 10.1002/adfm.201702946

a new avenue to convert light directly into useful work, contributing to the remote manipulation of various floating devices.

Although the abovementioned studies have already proven the feasibility of controlling devices through light-irradiation-induced surface tension gradients, some challenges remain, including the flexible integration of efficient photothermal materials, multifunctional structure design, and fluidic drag reduction. First, to tailor the local surface tension gradients and generate controllable motion, the device structures must be precisely designed, so that highly efficient photothermal materials should be well integrated with the device structures at any desired position.^[36,37] In this case, novel processing technologies that enable the designable patterning of both framework materials and photothermal materials are highly desirable. Additionally, the surface dewetting properties of these floating devices is another critical issue that should be considered. Since floating devices generally operate on a water surface, a solid–water–air three-phase interface is present, and obviously, water resistance acts on the devices when they move. To address this problem, superhydrophobic surfaces can be prepared at the solid–water–air three-phase interface. However, current reports on superhydrophobic light-driven floating devices that enable efficient light-to-work conversion remain rare. The difficulties in fabricating a functional layer that is both photothermally active and superhydrophobic are a possible reason for this gap.

In this work, we report the facile fabrication of light-driven superhydrophobic floating devices by direct laser writing (DLW) treatment on a slice of PDMS. Despite the fact that DLW technology has several limitations with respect to the spatial resolution (dominated by optical diffraction limit), limited processing materials and efficiency, DLW processing is quite promising for device fabrication since it enables flexible, mask-free patterning. Actually, any desired structures could be directly fabricated according to a preprogrammed patterns.^[38–40] More importantly, a simple laser treatment can carbonize the PDMS surface, naturally resulting in a highly efficient photothermal

layer with unique superhydrophobicity. By either integrating the functional layer at the desired position or designing asymmetric structures, floating devices such as a fish, a dozer boat, and rotating gears have been fabricated. These floating devices could be manipulated using different light sources including sunlight, a filament lamp, and a laser beam.

2. Results and Discussion

Laser processing has been proven to be a powerful technology that enables precise, programmable, position-selective fabrication both at the macro- and microscale. In this work, DLW was employed to finely tailor the shape of the device (**Figure 1a**) and to produce a light-absorption layer by surface modification (**Figure 1b**). Thus, arbitrarily shaped floating devices with well-defined geometries could be prepared in a facile one-step laser process, and the light-sensitive devices exhibited the potential to move on water under light irradiation (**Figure 1c**). Moreover, to drive the devices in a controlled manner, we could design devices with asymmetric contours and generate modified surfaces on the desired areas using DLW. As a typical example, we fabricated a gear-shaped PDMS device with an outer diameter of 15 mm using this method (**Figure 1d–f**). After modifying the surface using the laser engraving mode, the treated device turned black, which is beneficial for light absorption.

Importantly, for moving devices on water, water resistance is an inevitable and critical issue that is related to speed of movement and driving efficiency. Creating a superhydrophobic surface is an effective and promising method to reduce water resistance. It is well known that a superhydrophobic surface is generally obtained by combining rough structures with a low-surface-energy material. To fabricate a superhydrophobic surface, we chose PDMS for its hydrophobicity and commercial availability. However, the smooth pristine PDMS device was immediately immersed in water upon release (**Figure 2a**) due

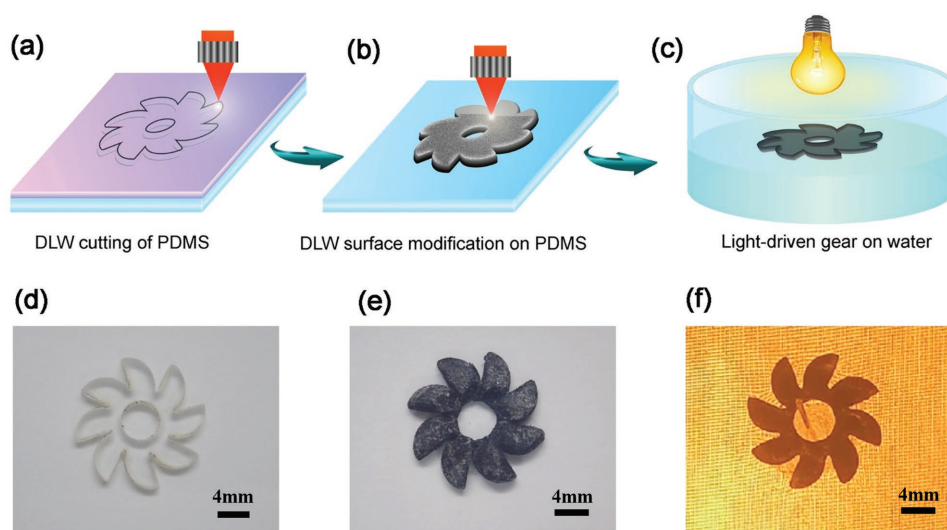


Figure 1. Schematic illustration of the fabrication and working processes of the superhydrophobic floating gears, including a) laser patterning, b) laser modification, c) and light-induced motion, and photographs of d) the patterned PDMS gear, e) surface-modified gear, and f) rotating gear driven by wide-field light.

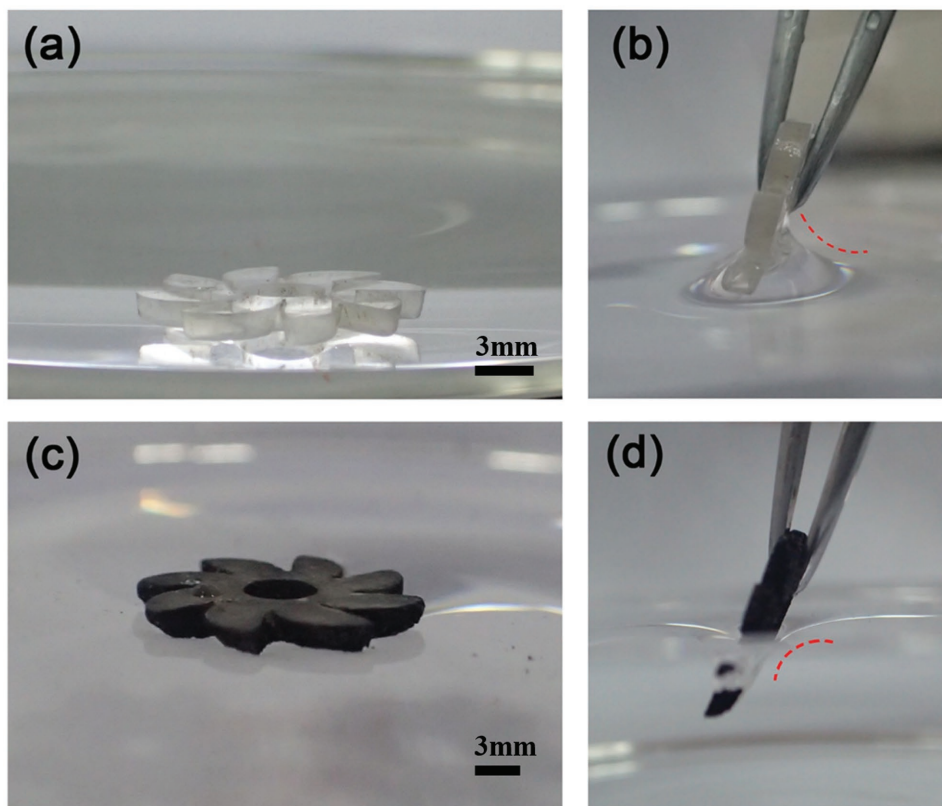


Figure 2. Wetting behaviors of the pristine and treated PDMS gear devices. a) Immersion of an untreated gear in water. b) Contact interface between an untreated gear and water. c) Floating of a treated gear on water. d) Contact interface between a modified gear and water.

to the adhesive interaction between water and pure PDMS, as indicated by the convex contact interface (Figure 2b). In this work, laser processing was employed for the surface modification of the PDMS structures. Interestingly, the laser-induced carbonization of the PDMS surface not only led to the formation of a black light-absorption layer but also made the surface very rough. Consequently, our laser-modified device became highly water repellent without an additional chemical treatment. As shown in Figure 2c, the laser-treated PDMS could float on water, benefiting from strong interfacial water repulsion and the resulting sufficient buoyancy (Figure 2d).

To characterize the wetting performance, we performed contact angle (CA) tests. A static CA as high as 153° was achieved, thus verifying the superhydrophobicity of our prepared device (Figure 3a). To investigate the formation mechanism of the surface superhydrophobicity, we further studied the structural and material properties of the surface. Scanning electron microscopy (SEM) images (Figure 3d) revealed the laser-induced micro-/nanostructures, which contributed to the hierarchical surface roughness. The confocal laser scanning microscope (CLSM) image (Figure 3b) revealed a gradient microstructure on the edge of the gear. The height profile (Figure 3c) showed that the height of the slope was 2 mm.

Following the surface modification, the pristine transparent PDMS turned black as the laser fluence increased, indicating the carbonization of PDMS. X-ray photoelectron spectroscopy (XPS) was performed to investigate the material features during

the laser treatment process. As shown in Figure 4a, the intensities of the C1s peaks significantly decreased, and those of the O1s peaks increased as the laser fluence increased, revealing precise control over the extent of carbonization. Notably, for pristine PDMS, the contents of carbon and oxygen atoms are $\approx 45.3\%$ and $\approx 27.9\%$, respectively. After laser modification, the carbon content decreased gradually, whereas the oxygen content increased, suggesting the carbonization process (Figure 4b). During the laser treatment, the methyl groups were carbonized first, and with the increasing laser intensity, more carbon was burnt away, accompanied by the emission of carbon species, leaving mainly silica. Therefore, the PDMS surface first turned black and then finally became white. In this case, the laser fluence should be optimized to control the surface wettability and the light absorption. According to our experimental results, when the carbon atom concentration of the carbonized layer reaches $\approx 33\%$, the surface would exhibit both superhydrophobicity and good light-absorption properties.

We further study the influence of laser fluence on the thickness of the laser treated layer. Generally, with the increase of laser fluence, the depth at the laser treated region increases quasi-linearly (Figure S1a, Supporting Information). However, the thickness of the as-formed layer does not show a similar tendency, a maximum value of ≈ 1.1 mm has been achieved under 9554 W cm^{-2} irradiation (Figure S1b, Supporting Information). We further calculate the yield of the fabrication by measuring the weight loss after laser treatment and the weight

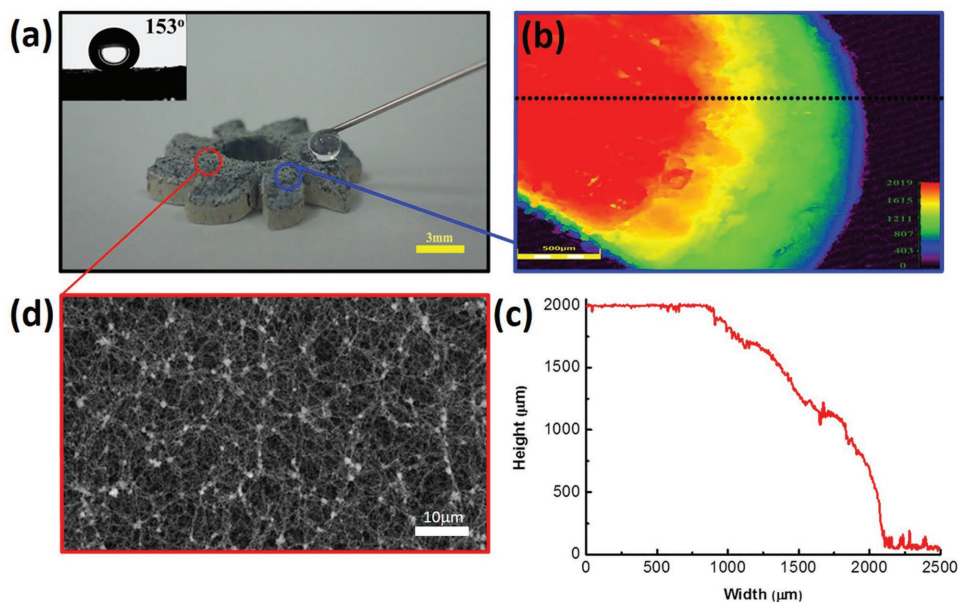


Figure 3. a) Photograph of the prepared gear device. The inset shows the water CA of the surface. b,c) 3D topography and height profile of a vane of the gear device, respectively. d) SEM image of the gear device.

of laser treated layer fabricated at this condition, a yield of $\approx 16\%$ has been achieved. When laser fluence is further increased, the decrease in thickness could be attributed to the laser ablation effect, in which carbon species has been burnt away under high laser fluence or multitudes treatments (Figure S1c, Supporting Information). In this regard, the thickness of the laser treated layer can be controlled by either laser fluence or laser treating time within a certain range.

In this work, we fabricated a series of PDMS samples under different laser fluences, and the effect of the laser fluence on the photothermal temperature increase under the same irradiation condition (0.9 W cm^{-2} , 10 s) was evaluated (Figure 5a). Generally, the laser-treated PDMS samples exhibited larger amplitudes than the pristine PDMS ($1.9 \text{ }^\circ\text{C}$). The temperature increase changed with the laser fluence, and a laser fluence of 9554 W cm^{-2} induced the largest temperature variation of

$14.3 \text{ }^\circ\text{C}$ in the sample. Thereafter, all light-driven devices were prepared under these conditions. To further evaluate the photothermal performance, we monitored the time-dependent change in the temperature for the pristine and laser-treated PDMS (laser fluence, 9554 W cm^{-2}). Following irradiation for 250 s, the temperature of the modified PDMS sharply increased from room temperature ($21.6 \text{ }^\circ\text{C}$) to $64 \text{ }^\circ\text{C}$, which was much higher than that of the pure PDMS (less than $40 \text{ }^\circ\text{C}$, Figure 5b). We further compared their photothermal effect in water. The temperature rise is slightly lower than that measured in air. Furthermore, the modified PDMS was demonstrated to have a high absorption capacity ($\approx 90\%$) for a wide range of wavelengths ranging from 240 to 1050 nm, while pure PDMS was almost transparent over this wavelength range (Figure 5c).

Exploiting the superhydrophobicity and photothermally active functional layers, we designed high-speed light-driven

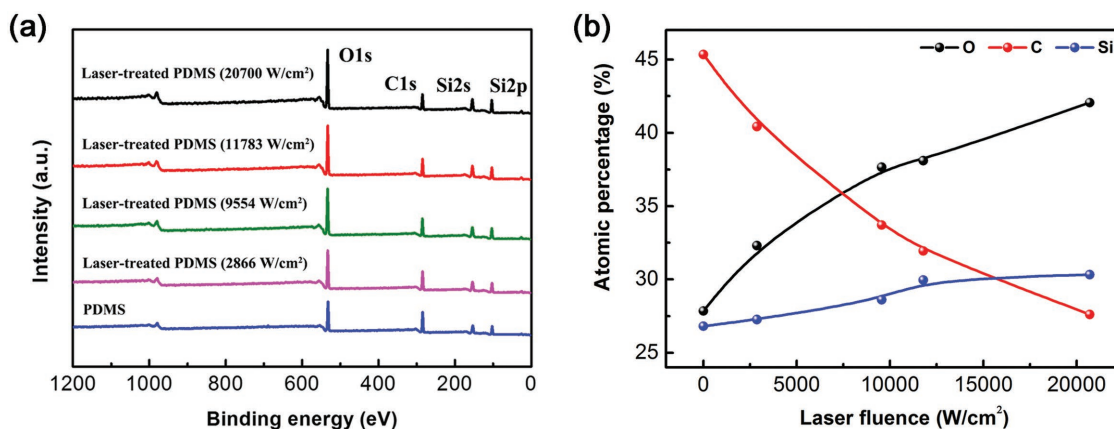


Figure 4. a) XPS spectra of the pristine and treated PDMS under different laser fluences. b) Dependence of the O, C, and Si atomic percentages on the laser fluence.

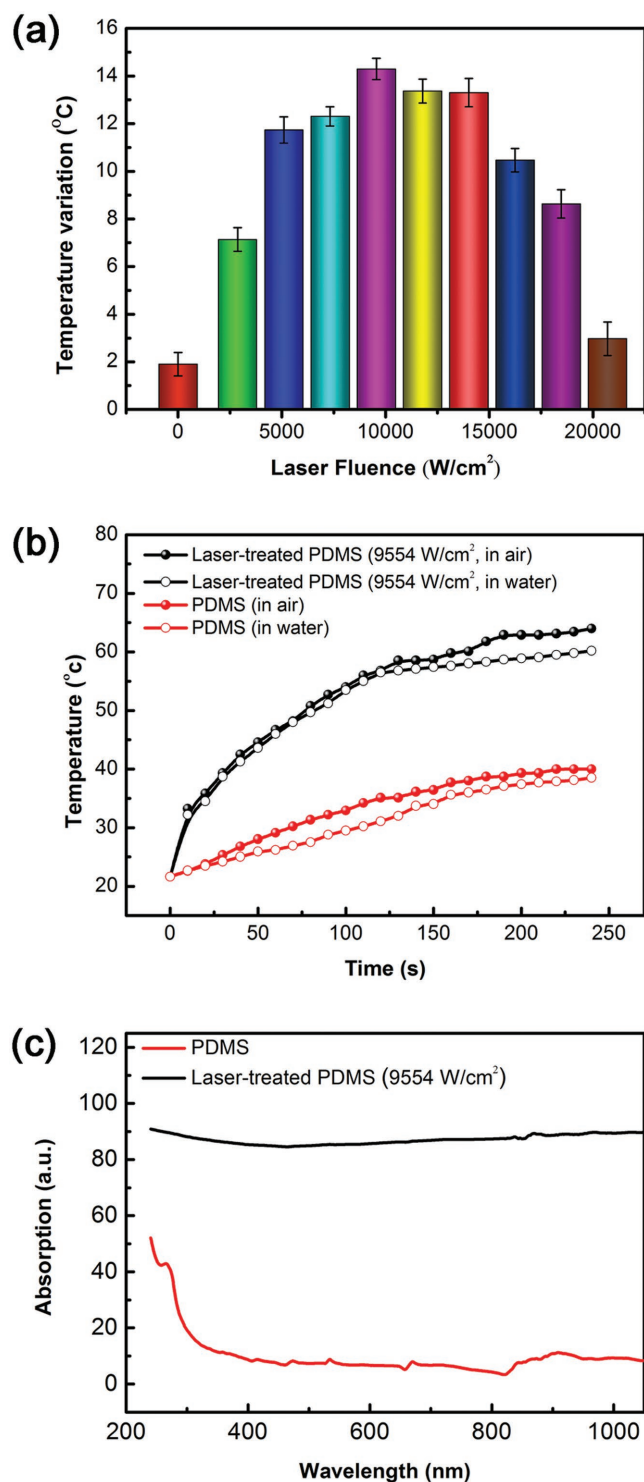


Figure 5. a) Dependence of the temperature increase of PDMS on the laser processing fluence under the same irradiation conditions ($\approx 0.9 \text{ W cm}^{-2}$, 10 s). b) Dependence of the surface temperature on irradiation time for the pristine and laser-treated PDMS measured in air and in water, respectively. c) Absorption spectra of the pristine and laser-treated PDMS (9554 W cm^{-2}).

actuators. Moreover, by constructing functional layers at desired positions, the devices could advance in a controllable manner. As an example, a dozer boat was prepared by

selectively modifying the rear and paw areas, as shown in **Figure 6a** (Videos S1 and S2, Supporting Information). Driven by laser irradiation, the boat could move directionally toward an object and push it to a specified location, as illustrated by the path of movement in **Figure 6a**. Here, the light induced pressure has also been considered (Supporting Information); which was calculated to be $6.7 \times 10^{-10} \text{ N}$. As compared with the gravity of the device (boat, $1.3 \times 10^{-5} \text{ N}$), the light pressure is neglectable. Since the light pressure is always perpendicular to the water surface, it would be conquered by the buoyance. In this regard, the light induced pressure do not show any influence on the driving performance. The direction of the linear motion could be manipulated by the irradiation position, where light-to-heat conversion was triggered and the local surface tension decreased with the increased temperature, leading to a nonzero driving force toward the light source. As mentioned above, our device enabled high absorption over a wide range of wavelengths. Accordingly, in addition to laser irradiation, focused sunlight could efficiently propel our device. As shown in **Figure 6b**, a model fish device with a laser-treated tail swam quickly and linearly under the irradiation of a focused sunlight beam.

Currently, most studies of light-driven macroscale devices require high-intensity sources (e.g., laser) because ordinary light generally cannot provide sufficient power. To address this problem, our strategy integrates a drag reduction layer and a light-absorption layer, making it possible to propel devices with ordinary light. Moreover, in addition to linear motion, rotational motion could be realized by designing asymmetric structures. For example, we designed a gear device with asymmetric vanes, each containing a curved side and a straight side, as shown in **Figure 7a**. Driven by a wide field of light, the gear device rotated counterclockwise at $\approx 1.57 \text{ rad s}^{-1}$, as indicated by the arrows in **Figure 7a** (Video S3, Supporting Information). Due to the structural features, the photogenerated heat distribution on this device was asymmetric. For each gear vane, the surface tension values on the two sides were different, thus causing the gear to rotate. As shown in **Figure 7b**, this strategy could be further extended to drive other unmodified gears by powering it with light (Video S4, Supporting Information).

To obtain further insights into the rotational motions described above, we investigated the mechanical model of the gear structure. Since surface tension plays a critical role in the interfacial activity and is influenced by the temperature, we performed infrared thermography to examine the temperature distribution of the asymmetric gear (**Figure 8a**). The light source was set at the center where the temperature was the highest, and the temperature gradually decreased radially. Due to the structural asymmetry of the gear vane, the green dot on the straight side and the blue dot on the curved side were isothermal (white dashed line). Therefore, the surface tensions at the green and blue dots were the same, as denoted by F2 (**Figure 8b**). According to the Harkins formula, the surface tension can be calculated as follows

$$e = b_0 + b_1 T + b_2 T^2 \quad (1)$$

where e is the surface tension (mN m^{-1}), $b_0 = 75.796 \text{ mN m}^{-1}$, $b_1 = -0.145 \text{ mN m}^{-1} \text{ }^\circ\text{C}^{-1}$, $b_2 = -0.00024 \text{ mN m}^{-1} \text{ }^\circ\text{C}^{-2}$, and

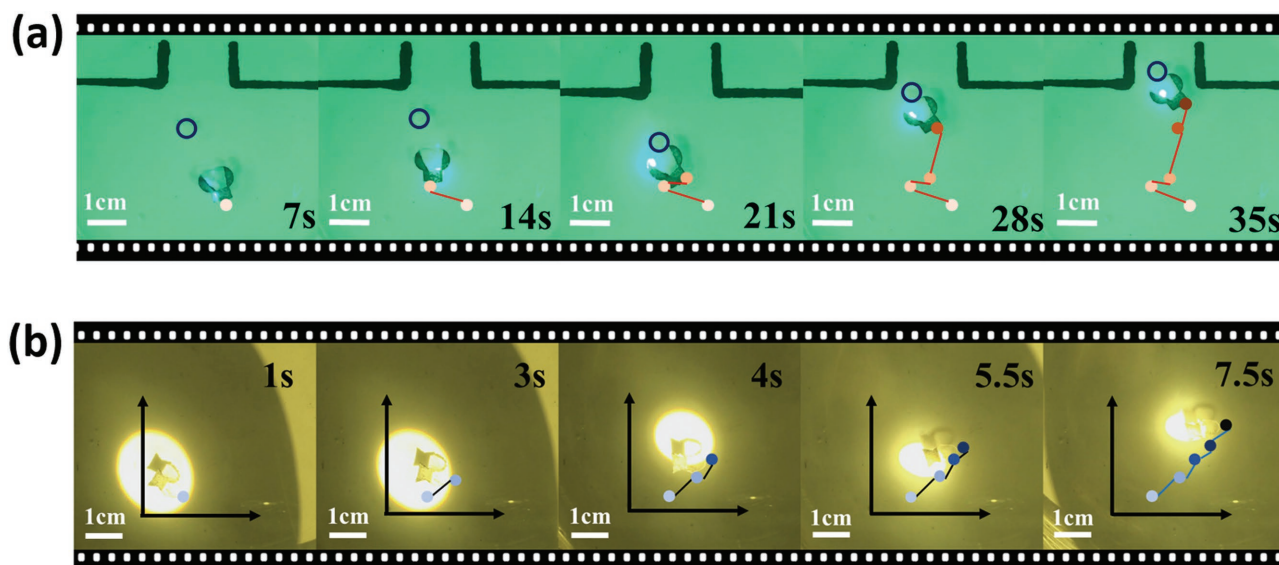


Figure 6. Light-driven linear motions of the superhydrophobic floating devices. a) Self-propelled boat for directional object transport under laser irradiation. It requires 1.5 s of continuous irradiation to drive the “boat.” b) Swimming fish device driven by sunlight. It requires 2.4 s of continuous irradiation to drive the fish. See Videos S1 and S2 of the Supporting Information.

T is the temperature ($^{\circ}\text{C}$). Because the surface tension always decreases with increasing temperature, surface tension in the relatively high temperature region would decrease more obviously. The force that generates the clockwise or counterclockwise rotation of the gear is perpendicular to the straight line connecting the center of the circle and the point of action. Here, we compared two pairs of typical sites with the same radius (green hollow/solid dots and blue solid/hollow dots). Typically, the surface tension is always perpendicular to the edge of the gear vane. Thus, the surface tension (F_2 and F_1) along the straight side of the gear is applied fully to produce clockwise angular momentum, while along the curved side,

only the decomposed force (F_3' and F_2') that is perpendicular to the straight line connected to the center contributes to the counterclockwise angular momentum to the gear. Obviously, the temperature of the hollow green dot at the curved side is much lower than that of the solid green dot with the same radius, and the solid blue dot is much cooler than the hollow blue dot. Therefore, the gear rotates counterclockwise if F_3' is larger than F_2 and F_2' is larger than F_1 . The disequilibrium of angular momentum leads to the rotation of the gear, and the key effect that causes this disequilibrium is the geometry-induced asymmetric temperature distribution of the gear.

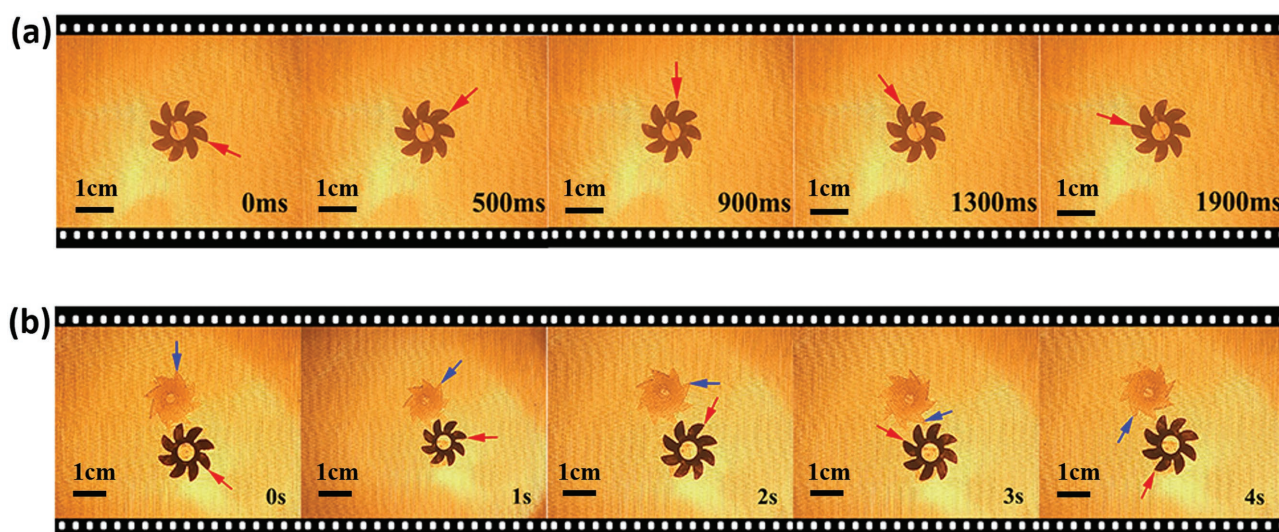


Figure 7. Light-driven rotational motions of the superhydrophobic floating devices. a) Active rotation of the gear device with asymmetric vanes under wide-field light irradiation, and b) resultant passive rotation of an untreated gear, which engages with the laser-treated gear device. It requires 6.6 s of continuous irradiation to drive the gear. See Videos S3 and S4 of the Supporting Information.

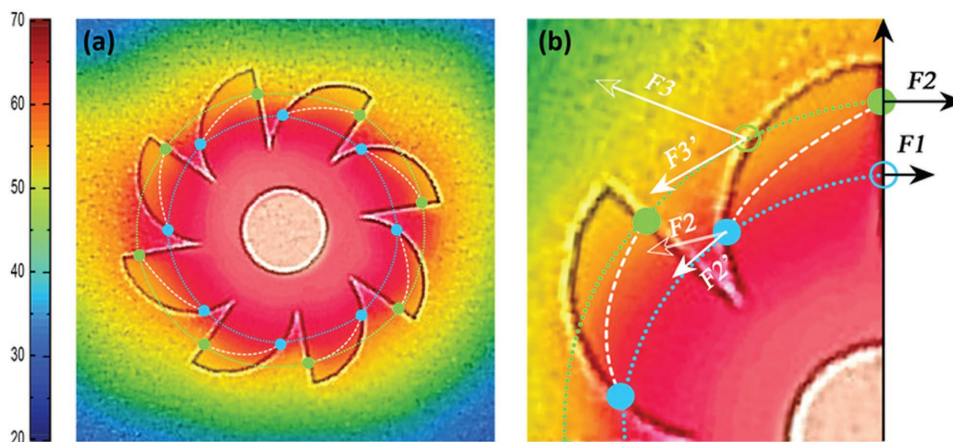


Figure 8. a) Thermography image of the rotating gear. b) Surface tension analysis of the gear.

3. Conclusion

Light-driven floating devices with a superhydrophobic, photo-thermal active layer are successfully prepared using a simple one-step method. The DLW technique is utilized to design devices with various shapes such as fish, dozer boat, and gear. To reduce the water resistance, microstructures are generated by laser engraving on the hydrophobic PDMS material, enabling unique superhydrophobicity and fast device motion. Additionally, laser treatment also leads to the carbonization of PDMS device and contributes to the high photothermal conversion capacity. By integrating the functional layer at the desired position or by designing asymmetric structures, linear or rotational motions are demonstrated. Furthermore, the resultant superhydrophobic devices are stable and reusable; they could be driven by a variety of light sources including sunlight, filament lamp, and laser beams. Our approach provides a simple, effective method for fabricating fast-moving floating devices and low-power light-driven actuators.

4. Experimental Section

Preparation of the Floating Devices: The devices were fabricated using a commercially available PDMS elastomer (Sylgard 184 Silicone Elastomer, Dow Corning Corporation). Typically, a PDMS prepolymer was mixed with a curing agent (10:1 by weight) and cured at 95 °C for 30 min. A 10 cm × 10 cm membrane was thus prepared for subsequent laser processing. A carbon dioxide laser engraving machine (JW6090, JG. Shandong) was used to pattern the device with programmable shapes and to separate it from the base materials (laser-cutting mode, 12738 W cm⁻²). Then, the patterned PDMS was laser treated (laser-engraving mode) for surface modification. To optimize the photothermal conversion performance, a series of laser fluences ranging from 2866 to 20700 W cm⁻² were investigated. The laser scanning speed is 100 mm s⁻¹ and the scanning step length is 0.03 mm. Thus, the fabrication efficiency is ≈1.8 cm² min⁻¹.

Characterization: SEM images were obtained using a JEOL field-emission scanning electron microscope (JSM-7500). The CA tests were made using a contact angle meter (SL200B, Solon Tech. Shanghai). XPS measurements were performed using an ESCALAB 250 spectrometer. CLSM images were obtained using an LEXT 3D measuring laser microscope (OLS4100). The temperatures were measured using a noncontact infrared thermometer (Smart Sensor AS872D). Thermal

images were obtained using an FLIR infrared thermal camera (FLIR One).

Supporting Information

Supporting Information is available from the Wiley Online Library or from the author.

Acknowledgements

The authors would like to acknowledge the National Natural Science Foundation of China and the Key Research and Development Program of China under Grant Nos. #61522503, #61376123, #61590930, #2017YFB1104300, and #2017YFB1104601.

Conflict of Interest

The authors declare no conflict of interest.

Keywords

direct laser writing, light driving devices, light-to-work conversion, photothermal surface tension effects, superhydrophobic surfaces

Received: June 1, 2017

Revised: July 24, 2017

Published online:

- [1] C. Maggi, F. Saglimbeni, M. Dipalo, F. De Angelis, R. Di Leonardo, *Nat. Commun.* **2015**, *6*, 7855.
- [2] Y. Hu, Z. Li, T. Lan, W. Chen, *Adv. Mater.* **2016**, *28*, 10548.
- [3] L. Soler, S. Sanchez, *Nanoscale* **2014**, *6*, 7175.
- [4] Y. He, S. Liao, H. Jia, Y. Cao, Z. Wang, Y. Wang, *Adv. Mater.* **2015**, *27*, 4622.
- [5] O. A. Araromi, S. Rosset, H. R. Shea, *ACS Appl. Mater. Interfaces* **2015**, *7*, 18046.
- [6] K. Malachowski, M. Jamal, Q. Jin, B. Polat, C. J. Morris, D. H. Gracias, *Nano Lett.* **2014**, *14*, 4164.

- [7] Y. Tian, Y. L. Zhang, J. F. Ku, Y. He, B. B. Xu, Q. D. Chen, H. Xia, H. B. Sun, *Lab Chip* **2010**, *10*, 2902.
- [8] W. Jiang, D. Niu, H. Liu, C. Wang, T. Zhao, L. Yin, Y. Shi, B. Chen, Y. Ding, B. Lu, *Adv. Funct. Mater.* **2014**, *24*, 7598.
- [9] N. Hu, X. Han, S. Huang, H. M. Grover, X. Yu, L. N. Zhang, I. Trase, J. X. Zhang, L. Zhang, L. X. Dong, Z. Chen, *Nanoscale* **2017**, *9*, 2958.
- [10] Y. Zhao, Q. Han, Z. Cheng, L. Jiang, L. Qu, *Nano Today* **2017**, *12*, 14.
- [11] J. Zhang, L. Song, Z. Zhang, N. Chen, L. Qu, *Small* **2014**, *10*, 2151.
- [12] M. J. Villangca, D. Palima, A. R. Bañas, J. Glückstad, *Light: Sci. Appl.* **2016**, *5*, e16148.
- [13] T. Wang, J. Huang, Y. Yang, E. Zhang, W. Sun, Z. Tong, *ACS Appl. Mater. Interfaces* **2015**, *7*, 23423.
- [14] Z. Cheng, T. Wang, X. Li, Y. Zhang, H. Yu, *ACS Appl. Mater. Interfaces* **2015**, *7*, 27494.
- [15] J. Huang, H. Zhang, X. Yan, L. Zhang, *Nanomedicine* **2016**, *12*, 488.
- [16] S. Kim, S. Lee, J. Lee, B. J. Nelson, L. Zhang, H. Choi, *Sci. Rep.* **2016**, *6*, 30713.
- [17] T. Xu, J. Yu, X. Yan, H. Choi, L. Zhang, *Micromachines* **2015**, *6*, 1346.
- [18] K. Kumar, C. Knie, D. Bleger, M. A. Peletier, H. Friedrich, S. Hecht, D. J. Broer, M. G. Debije, A. P. Schenning, *Nat. Commun.* **2016**, *7*, 11975.
- [19] D. Okawa, S. J. Pastine, A. Zettl, J. M. J. Fréchet, *J. Am. Chem. Soc.* **2009**, *131*, 5396.
- [20] Y. Zhao, L. Song, Z. Zhang, L. Qu, *Energy Environ. Sci.* **2013**, *6*, 3520.
- [21] H. Xing, J. Li, Y. Shi, J. Guo, J. Wei, *ACS Appl. Mater. Interfaces* **2016**, *8*, 9440.
- [22] D.-D. Han, Y.-L. Zhang, Y. Liu, Y.-Q. Liu, H.-B. Jiang, B. Han, X.-Y. Fu, H. Ding, H.-L. Xu, H.-B. Sun, *Adv. Funct. Mater.* **2015**, *25*, 4548.
- [23] H. Cheng, Y. Hu, F. Zhao, Z. Dong, Y. Wang, N. Chen, Z. Zhang, L. Qu, *Adv. Mater.* **2014**, *26*, 2909.
- [24] O. Lecarme, Q. Sun, K. Ueno, H. Misawa, *ACS Photonics* **2014**, *1*, 538.
- [25] B.-B. Xu, L. Wang, Z.-C. Ma, R. Zhang, Q.-D. Chen, C. Lv, B. Han, X.-Z. Xiao, X.-L. Zhang, Y.-L. Zhang, K. Ueno, H. Misawa, H.-B. Sun, *ACS Nano* **2014**, *8*, 6682.
- [26] A. S. Bezryadina, D. C. Preece, J. C. Chen, Z. Chen, *Light: Sci. Appl.* **2016**, *5*, e16158.
- [27] K. Watanabe, H. Hayasaka, T. Miyashita, K. Ueda, K. Akagi, *Adv. Funct. Mater.* **2015**, *25*, 2794.
- [28] S. G. Hahm, T. J. Lee, M. Ree, *Adv. Funct. Mater.* **2007**, *17*, 1359.
- [29] H. He, X. Zheng, J. Zhang, S. Liu, X. Hu, Z. Xie, *J. Mater. Chem. B* **2017**, *5*, 2491.
- [30] L. Yang, J. Cheng, Y. Chen, S. Yu, F. Liu, Y. Sun, H. Ran, *Sci. Rep.* **2017**, *7*, 45213.
- [31] J. Guo, T. Oshikiri, K. Ueno, X. Shi, H. Misawa, *Anal. Chim. Acta* **2017**, *957*, 70.
- [32] B. Wang, Y. Zhang, L. Zhang, *Nanoscale* **2017**, *9*, 4777.
- [33] S.-Y. Tang, V. Sivan, P. Petersen, W. Zhang, P. D. Morrison, K. Kalantar-zadeh, A. Mitchell, K. Khoshmanesh, *Adv. Funct. Mater.* **2014**, *24*, 5851.
- [34] X. Li, T. Yang, Y. Yang, J. Zhu, L. Li, F. E. Alam, X. Li, K. Wang, H. Cheng, C.-T. Lin, Y. Fang, H. Zhu, *Adv. Funct. Mater.* **2016**, *26*, 1322.
- [35] O. A. Louchev, S. Juodkazis, N. Murazawa, S. Wada, H. Misawa, *Opt. Express* **2008**, *16*, 5673.
- [36] J. Wang, J. Zhao, Y. Li, M. Yang, Y.-Q. Chang, J.-P. Zhang, Z. Sun, Y. Wang, *ACS Macro Lett.* **2015**, *4*, 392.
- [37] Y. Cao, J.-H. Dou, N.-j. Zhao, S. Zhang, Y.-Q. Zheng, J.-P. Zhang, J.-Y. Wang, J. Pei, Y. Wang, *Chem. Mater.* **2017**, *29*, 718.
- [38] V. Mizeikis, *J. Laser Micro/Nanoeng.* **2014**, *9*, 42.
- [39] Y.-L. Sun, W.-F. Dong, L.-G. Niu, T. Jiang, D.-X. Liu, L. Zhang, Y.-S. Wang, Q.-D. Chen, D.-P. Kim, H.-B. Sun, *Light: Sci. Appl.* **2014**, *3*, e129.
- [40] M. Schumann, T. Bückmann, N. Gruhler, M. Wegener, W. Pernice, *Light: Sci. Appl.* **2014**, *3*, e175.